

# 3D City Map Reconstruction from UAV-based Radio Measurements

Omid Esrafilian, David Gesbert<sup>1</sup>

Communication Systems Department, EURECOM, Sophia Antipolis, France  
Email: {esrafilian, gesbert}@eurecom.fr

**Abstract**— This paper considers the problem of 3D city map reconstruction. The key novelty here lies in the sole exploitation of UAV-bound radio measurements as a way to recover the map data, i.e. no image of the city is taken or processed. The proposed approach relies on the unique ability for a UAV-to-ground communication system to detect and classify line-of-sight (LoS) vs. non line-of-sight (NLoS) channels towards ground users using machine learning tools. Once classification is carried out, the LoS vs. NLoS data is fed as input to a building position and height reconstruction algorithm. The map reconstruction quality is analyzed as a function of user density and UAV altitude, revealing the notion of an optimal height for the UAV which is predicted using an analytical model.

**Keywords**— UAV; drone; city map; channel modeling; machine learning, classification; learning.

## I. INTRODUCTION

The problem of 3D city map reconstruction has key applications in a wide range of both non-communications (facility and utility managements, city planning, navigation etc.) as well as communications-related areas (e.g. radio engineering, base station deployment planning, channel quality and coverage prediction etc.). Traditionally, 3D city map reconstruction uses photogrammetry techniques which need high resolution stereo images and extensive processing capability [1]. Over the past decade, a number of approaches have been developed which employ remote sensing techniques for obtaining geometry measurements of the environment using depth information [2]. In all former methods, the 3D map of the city is driven by trying to fit some kinds of synthetic building models into the obtained data. Additional studies have been conducted related to 3D object reconstruction which are based on capturing the shadow of an object from multiple views [3].

In an apparently completely independent thread of technology, the exploitation of drones, a.k.a UAV (Unmanned Aerial Vehicles) at various ranges of altitudes for future wireless cellular communication networks has recently gain significant attention [4, 5]. The use of lightweight low-altitude UAV is very attractive as it provides a quickly deployable relay functionality in weakly covered areas, temporary hotspot areas, or as an alternative to expensive terrestrial ultra-dense networks. While existing work on the use of UAV in radio access networks has focused on the problem of optimal UAV positioning [6, 7], and radio capacity maximization [8] or radio map predictions [9, 10],

its potential interest as a tool to reconstruct 3D city maps, from the radio measurements it can make, has so far been completely overlooked. Hence this paper constitutes a first attempt at it. Note that another motivation for reconstructing 3D maps using a drone lies in the fact that the 3D map itself can be exploited as a tool to enhance the solution to optimally positioning the very same drone in networking applications [18]. The proposed principle of reconstructing building shapes and locations from radio measurements bears some intuitive analogy with the problem of reconstructing the shape of an object that is exposed under a series of light sources from the shadow images created from the object. Some major differences are to be noted however. In our context, the light/shade classification is replaced with a notion of LoS/NLoS classification for the radio channel. However, a major challenge lies in the fact that the LoS/NLoS data is not readily available from the measurement data itself. Or rather this information must somehow be inferred from the measurements via a learning algorithm which is proposed in the paper. Secondly, the reconstruction of the very rich topology information of a city with hundreds of building is much more difficult than that of most common objects. Luckily, this problem is compensated by (i) the fact that the UAV can be tuned to record channel measurement from a very large number of ground user locations within a short time span, and (ii) the UAV positions can be modified and cumulated to offer a rich data set for learning, and ultimately giving an accurate description of the ground terrain. It should be noted that the notion of using signal strength measurements for characterizing the shape of a building is not new in itself. In [19] the authors propose the use of satellite-based GPS measurement to enhance 3D maps. However, the use of satellite is not as flexible as that of drones as their path cannot be optimized. Also in [20] propose the use of two drones to infer the inner structure of a building.

In summary, our contributions in this paper are as follows:

- We propose a first attempt for reconstructing a whole 3D city map based on radio measurements made from a low altitude UAV with receive signal strength indicator (RSSI) sensing capability. The RSSI levels are gathered at each selected UAV location from a large set of static outdoor ground users in a time-division multiplexing mode (TDM).
- The approach consists of two phases. In phase 1, machine learning tools are applied to learn the propagation parameters from the RSSI measurements from a target group of ground users. The learned parameters are in turn exploited to classify outdoor users in either LoS or NLoS

<sup>1</sup> This work is supported by the ERC under the European Union's Horizon 2020 research and innovation program (Agreement no. 670896).

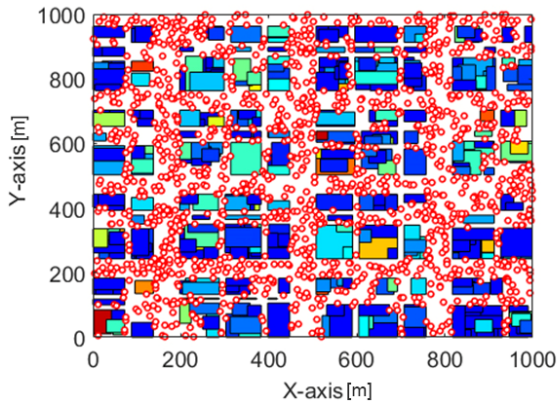


Fig. 1. Top view of the city building map and outdoor ground user locations which are shown by circles.

categories. A technique is proposed to optimize the selection of the target user group. In phase 2, the LoS/NLoS classified data is exploited to yield a reconstructed city map via the low-complexity resolution of a large set of inequality equations. Note that this paper tackles the case of hard LoS/NLoS classification. The scenario of soft (probabilistic) LoS classification is studied in a companion work by the same authors.

- Finally, the reconstruction quality reveals the notion of an optimal UAV altitude which is predicted analytically using an abstracted city model.

## II. SYSTEM AND CHANNEL MODELS

### A. System Model

We consider an urban area randomly uniformly scattered with a (possibly large) set of  $N$  ground level users carrying radio transmitting equipment. All the users of interest are assumed to be outdoor users and surrounded by a number of city buildings as illustrated in Fig. 1. Note that indoor users could potentially be exploited to improve reconstruction although this aspect is left for follow-up work. The city takes the shape of a square with length  $L$ . The true city map is drawn according to a random model where streets follow a Manhattan-like regular grid and building heights follow a bounded random distribution (see details in simulation section). The width of each building is random uniform with average  $W$ . The main street width is set to  $V$  (some lanes can be smaller). An UAV flies over the city, following a prescribed arbitrary trajectory, in order to measure the signal strength from the  $N$  users (while possibly providing connectivity services) which have GPS-tracked 2D positions denoted by  $X_U^i = (x_U^i, y_U^i) \in \mathbb{R}^2, i = 1 \dots N$ . Over the course of its trajectory, the UAV collects  $N \cdot K$  scalar RSSI measurements where  $K$  is the number of UAV locations at which multi-user measurements are made. In particular the RSSI from the  $i$ -th user at the  $k$ -th UAV location  $X_D^k$  is denoted by  $\gamma(X_U^i, X_D^k)$ . The 3D  $k$ -th UAV location is denoted by  $X_D^k = (x_D^k, y_D^k, H_D) \in \mathbb{R}^3, k = 1 \dots K$  where  $H_D$  is a fixed selected flying altitude (see section V).

### B. Channel Model

The air-to-ground mobile channel has been studied extensively in the recent years (see for instance [11, 12]).

Classically the channel gain between user and the UAV in dB is modeled as

$$\gamma_S = \beta_S - 10\alpha_S \log_{10} d + \xi_S \quad (1)$$

Where  $\alpha_S$  is the path loss exponent,  $d$  is the distance between the transmitter (ground user) and the receiver (UAV),  $\beta_S$  is the average channel gain at a reference point, and  $\xi_S$  models the shadowing effect which is considered as a Gaussian random variable  $\mathcal{N}(0, \sigma_S^2)$ . The subscript  $S$  (for “state”) emphasizes the strong dependence of the propagation parameters on the LoS or NLoS nature of the channel [15]. Hence we have two states:  $S=$ “LoS” or  $S=$ “NLoS”. This dependency is exploited in the first phase of our approach which focuses on LoS/NLoS classification for all ground users. It is important to note that we do not differentiate among NLoS channels according to how many buildings must be penetrated by the LoS direction to reach the receiver, although finer channel models may in principle allow to exploit this additional information for further improvements.

## III. LoS VS. NLoS CLASSIFICATION

Similar to detecting “shade” vs. “light” in an image, we propose to determine and exploit the LoS vs. NLoS status of any drone-user link. To this end, we adapt classical Support Vector Machine (SVM)-based machine learning methods to classify the users in LoS and NLoS categories from each UAV position  $X_D^k, k = 1 \dots K$ . In turn, maximum likelihood estimator (MLE) will be employed to find the parameters of each LoS and NLoS channel model. Note that classification requires a labeled training data set which is not available in our setting, hence some unsupervised learning is required. However, in order to reduce complexity, we propose to apply unsupervised learning (in the form of K-means clustering) over a selected target group of users rather than on the entire network. Our simulations suggest that a satisfactory performance for channel parameter estimation can be reached this way. An approach for optimizing the selection of the target user group is later proposed.

### A. Target User Clustering

We consider a fixed UAV location<sup>1</sup>  $X_D$  and a target subgroup of users, defined by the area located in a ring centered at the UAV with radius  $R$  and a width  $\Delta R$ . The value of  $\Delta R$  can be adjusted to control the target population size. The target user group is selected as a (narrow) ring in order to maximize distinguishability between LoS and NLoS effects on RSSI, while abstracting out the distance effect on path loss. In turn, the target users are clustered into LoS and NLoS categories based on the measured RSSI using a standard K-means approach [13].

### B. Optimization of Target User Group

Since the clustered target users will serve as labeled training data to classify the rest of the network users, it is essential that maximum LoS/NLoS distinguishability is achieved on the target group. The following method is proposed for selecting the ring radius  $R$ .

Let  $n_{LoS}(R)$  and  $n_{NLoS}(R)$  be the number of users in LoS and NLoS categories after clustering. Also let  $\bar{\gamma}_{LoS}(R)$ ,

<sup>1</sup>  $X_D$  can coincide with  $X_D^1$  or be a default location such as the center of the network.

$\bar{\gamma}_{NLoS}(R)$  be the average RSSI measured over the users in the LoS and NLoS clusters respectively. The following criterion  $J(R)$  attempts to strike a trade-off between the distinguishability between the RSSI of LoS and NLoS channels which is typically seen at larger distances, and the balance in LoS vs. NLoS population sizes which is observed from the UAV at closer distances. Indeed for a fixed UAV altitude, the users located at a greater distance from the UAV will all tend into the NLoS category. The criterion is selected as:

$$J(R) = \left( \frac{\min(n_{LoS}(R), n_{NLoS}(R))}{n_{LoS}(R) + n_{NLoS}(R)} * |\bar{\gamma}_{LoS}(R) - \bar{\gamma}_{NLoS}(R)| \right)^{-1} \quad (2)$$

Inverse of  $J(R)$  can be interpreted as an approximation of the average RSSI difference between LoS and NLoS users in the target group. The appropriate  $R$  can be found by optimizing the following expression using a discretized line search:

$$R^* = \arg \min_R J(R) \quad (3)$$

### C. Radio Propagation Parameter Learning

Considering the clustered RSSI measurements, which are generated from section III.A, we now want to estimate the propagation parameters for each of the LoS and NLoS scenarios. Considering  $d^i$  the distance of  $i$ -th user in the target group from the UAV, hence the RSSI for target user  $i$  with LoS/NLoS status  $S$  can be modeled as

$$\gamma_S^i = \beta_S - \alpha_S \varphi(d^i) + \xi_S \quad (4)$$

where  $\varphi(d) = 10 \log_{10} d$ . Due to the Gaussianity of  $\xi_S$ , the distribution of RSSI conditioned on status  $S$  can be written as

$$p(\gamma_S^i | d^i; \theta_S) = \frac{1}{\sqrt{2\pi\sigma_S^2}} \exp\left(-\frac{(\gamma_S^i - \beta_S + \alpha_S \varphi(d^i))^2}{2\sigma_S^2}\right) \quad (5)$$

where  $\theta_S = \{\alpha_S, \beta_S, \sigma_S\}$ . Therefore, assuming the estimated LoS/NLoS labels are perfect, the likelihood function of parameters  $\theta_S$  for each cluster is denoted by

$$L(\theta_S) = p(\bar{\gamma}_S | \vec{d}; \theta_S) = \prod_{i=1}^{n_S} p(\gamma_S^i | d^i; \theta_S) \quad (6)$$

where  $n_S$  is the number of users in each cluster (LoS or NLoS). Then the maximum likelihood estimation (MLE) [14] can be obtained from solving the following optimization problem

$$\max_{\theta_S} \prod_{i=1}^{n_S} p(\gamma_S^i | d^i; \theta_S) \quad (7)$$

or equivalently instead maximizing the log likelihood  $\ell(\theta_S)$

$$\begin{aligned} \ell(\theta_S) &= \log L(\theta_S) = \sum_{i=1}^{n_S} \log p(\gamma_S^i | d^i; \theta_S) \\ &= n_S \log \frac{1}{\sqrt{2\pi\sigma_S^2}} - \frac{1}{2\sigma_S^2} \sum_{i=1}^{n_S} (\gamma_S^i - \beta_S + \alpha_S \varphi(d^i))^2 \end{aligned} \quad (8)$$

This function can be maximized by differentiating with respect to the  $\theta_S = \{\alpha_S, \beta_S, \sigma_S\}$  and setting to zero (more details can be found in [9]).

### D. User Classification

Equipped with estimates of the propagation parameters, we proceed with classifying the remaining network users into LoS or NLoS categories. Several methods can be resorted to. In this paper, we use the SVM classifier for the sake of good performance, robustness and ease of implementation [15].

Considering the clustered RSSI observations obtained from section III.A as training data set  $\mathcal{T}(f^j, t^j | j = 1, 2, \dots, n_{LoS}(R) + n_{NLoS}(R))$  where  $f^j$  is the input feature and  $t^j$  corresponds to a LoS/NLoS label for the  $j$ -th user in the target group. We define  $f^j$  as

$$f^j = \|\gamma^j - \hat{\gamma}_{LoS}^j\|_2, \quad t^j = \begin{cases} 1 & LoS \\ -1 & NLoS \end{cases} \quad (9)$$

In (9)  $\gamma^j$  denotes measured RSSI and  $\hat{\gamma}_{LoS}^j$  is the predicted RSSI under a LoS channel hypothesis. Now armed with defined training data set  $\mathcal{T}$ , a SVM machine learning algorithm is designed to classify the users. We define

$$t(f) = \text{sign}(\omega^T \psi(f) + \omega_0) \quad (10)$$

Where  $\psi(f)$  is the predetermined input feature mapping function and  $(\omega, \omega_0)$  are parameters learned from the training data. As feature mapping function the Radial Basis Function (RBF) is classically selected [16]. We apply (10) for every network user to find its LoS/NLoS label.

Note that the above algorithm treats each user independently. As a way to save on complexity or improve robustness it is possible to exploit the natural correlation in the LoS/NLoS status for users that are closely located. This can be easily implemented by discretizing the map into small grid squares (few meters) and assigning all users in the same grid squares to a unique status (e.g. determined from majority rule)

## IV. 3D CITY MAP RECONSTRUCTION

In order to carry out the map reconstruction, we discretize the city and represent it in the form of a grid map where each grid element consists of 2D coordinates and a height indicator which will serve as an estimate of the height for any building located as these coordinates. The height indicator of the all grids are initialized equal to the maximum possible building height  $H_{Max}$ , and then iteratively refined using LoS status information.

### A. Map Reconstruction

The  $i$ -th element of the grid for the reconstructed map is denoted by  $\hat{g}_i = (x_i, y_i, \hat{z}_i)$  where  $\hat{z}_i$  denotes the building height estimate at ground coordinates  $(x_i, y_i)$ . In contrast, the true map's grid is defined as  $g_i = (x_i, y_i, z_i)$ . Note that by construction  $\hat{z}_i \geq 0$ ,  $z_i \geq 0$  and  $z_i = 0$  points to a street location.

In our approach we *iteratively* solve for  $\hat{z}_i$  for all  $i$ , by working out the sequence of inequalities implied by the existence of labels set to LoS pertaining to users that are informative of the  $i$ -th grid. As an illustration, let us take the example of one user at location  $X_U = (x_U, y_U)$  and the UAV located at  $X_D = (x_D, y_D, H_D)$ . The equation of the 3D line which passes through these two points is given by

$$\mathcal{L}: \frac{x-x_D}{x_U-x_D} = \frac{y-y_D}{y_U-y_D} = \frac{z-H_D}{-H_D} \quad (11)$$

Let  $\hat{G} = \{\hat{g}_1, \hat{g}_2, \dots, \hat{g}_n\}$  be defined as the set of grids which lie on projection of the line  $\mathcal{L}$  onto X-Y plan. Assuming this user-drone link has a LoS label, we can write a set of inequalities for all  $\hat{g}_i$  as follows

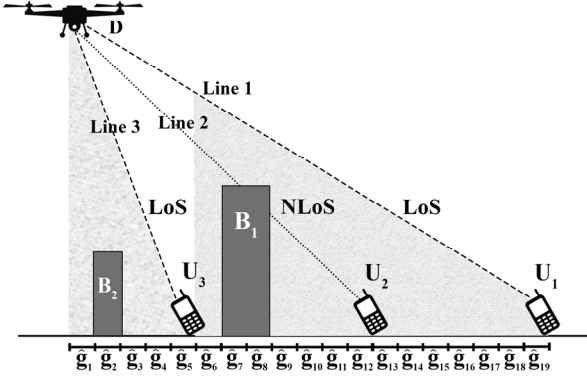


Fig. 2. Building map reconstruction: Example with 3 RSSI measurements. The first and third users were successfully labeled as LoS, while the second was correctly labeled NLoS. As a result any building between the drone and user 1 (resp. user 3) must lie below line 1 (resp. below line 3).

$$\hat{z}_i \leq \frac{(x_i - x_D)(-H_D)}{x_U - x_D} + H_D ; \forall \hat{g}_i \in \hat{G} \quad (12)$$

---

**Algorithm 1** Pseudocode for map reconstruction

---

```

1: Initialize the height of all grids to  $H_{Max}$ 
2: For  $k \in K$  then
3:   For  $i \in N$  then
4:     If  $X_U^i$  is LoS then
5:        $\mathcal{L} \leftarrow$  3D line passes through  $(X_D^k, X_U^i)$ 
6:        $\mathcal{L}_{Prj} \leftarrow$  Projection of  $\mathcal{L}$  on the ground
7:        $\hat{G}^i \leftarrow$  Grids which are on the  $\mathcal{L}_{Prj}$  line
8:       For  $j \in \hat{G}^i$  then
9:          $h_j = \frac{(x_j^i - x_D^k)(-H_D)}{x_U^i - x_D^k} + H_D$ 
10:         $\hat{z}_j^i := \min\{\hat{z}_j^i, h_j\}$ 
11:        If  $\hat{z}_j^i < H_{Min}$  then
12:           $\hat{z}_j^i = 0$  (street location)
13:        End if
14:      End
15:    End if
16:  End
17: End

```

---

The value in the right side of (12) corresponds to the  $z$  value of line  $\mathcal{L}$  in the center of  $i$ -th grid  $(x_i, y_i)$ . To put it differently, all the buildings along the line  $\mathcal{L}$  must lie below it as illustrated in Fig. 2. After accounting for inequality (12)  $\hat{z}_i$  is updated with  $\min(\hat{z}_i, \frac{(x_i - x_D)(-H_D)}{x_U - x_D} + H_D)$ . Moreover, we assume that all the building in the city are taller than a min value  $H_{Min}$ , therefore the grids with final height estimates lower than  $H_{Min}$  are set to zero and considered as street locations.

Inequalities (12) are solved for all given pairs of users and UAV locations where measurements are gathered. Clearly the map reconstruction performance highly depends on the trajectory  $D = \{X_D^1, \dots, X_D^K\}$  followed by the UAV to produce a rich enough measurement data set. The problem of optimizing for the UAV path is omitted and studied in an upcoming companion paper for space reasons. In this paper a simple yet reasonable path planning is considered (see Section V).

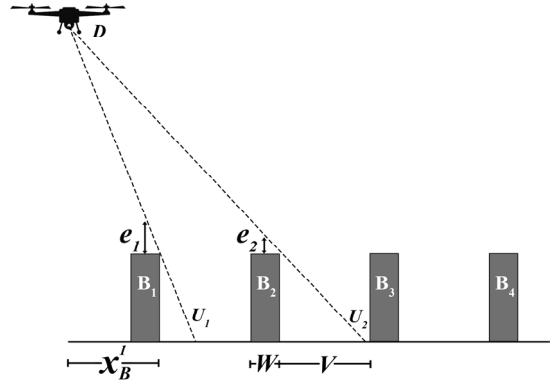


Fig. 3. One dimensional simplified deterministic city model.

### B. Optimum UAV Altitude

Although it is clear from intuition that the selection of a particular UAV altitude  $H_D$  impacts the map reconstruction performance, the derivation of an exact optimum is bound to be difficult, depending on many system parameters. Nevertheless our studies reveal two major factors in driving reconstruction performance. First an overly low flight height yields an excess in the number of NLoS reported measurements. Such measurements are less informative about the city topology than LoS reportings because they characterize the existence of some building *somewhere* crossing the line of sight but without a mention of *where*. In contrast, flying too high on the other hand will cause a gross overestimation of building heights ( $\hat{z}_i = H_{Max} \forall i$ ). In this section we build a small analytical deterministic model which captures these key effects so as to provide a guideline to design  $H_D$ . Interestingly, the trade-off above governing the choice of an optimum altitude is captured by a simplified one-dimensional city model with a continuum of outdoor users and where all the buildings are of equal length  $W$  and equal height the inter building space of  $V$  and the city map side of  $L$ . All buildings are set to a height matching that of the average in the true city  $H_{Av}$ , yet assumed unknown here. We consider a single UAV location with height  $H_D$ . When modeling the reconstruction error it is assumed that the building height is unknown but only the upper bound  $H_{Max}$  is known. After processing the LoS-based inequalities, the reconstruction error can be written as shown below.

*Proposition 1:* The reconstruction error after accounting for LoS-based inequalities is as follows

$$E_T(H_D) = \left( \left\lfloor \frac{L}{W+V} \right\rfloor - M \right) \cdot (H_{Max} - H_{Av}) + \sum_{j=1}^M \frac{W \cdot (H_D - H_{Av})}{2j(W+V)} \quad (13)$$

Where  $M = \left\lfloor \frac{V \cdot (H_D - H_{Av})}{H_{Av} \cdot (W+V)} \right\rfloor$  and  $\lfloor \cdot \rfloor$  denotes the floor function.

*Proof:* A sketch of proof is now given. Referring to the illustration shown in Fig. 3, we consider the subset of buildings for which there exists a LoS user whose line connecting to the UAV is tangent to the right top corner of the building. We denote by  $M = \left\lfloor \frac{V \cdot (H_D - H_{Av})}{H_{Av} \cdot (W+V)} \right\rfloor$  the number of such buildings which is derived from the position of farthest LoS tangent user from the

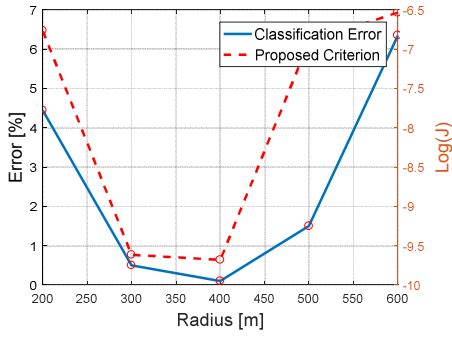


Fig. 4. Determining the best radius of the ring-like area for K-means algorithm using proposed criterion. Solid line denotes the classification error for each radius and dashed line is the corresponding criterion, predicting the same minimum.

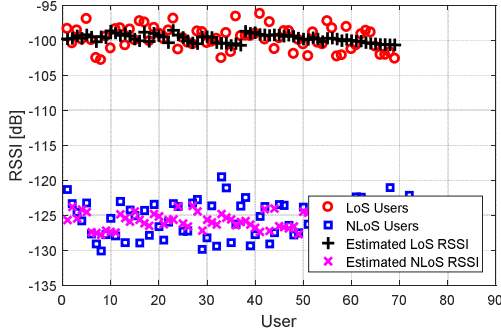


Fig. 5. K-means result for measured RSSI for users in target area and estimated RSSI for them using MLE.

UAV ( $U_2$  in Fig. 3). Note that for the  $j$ -th such building, a height estimate can be obtained given by

$$\hat{z}_j = \frac{2x_B^j H_{Av} + W \cdot (H_D - H_{Av})}{2x_B^j} \quad (14)$$

where  $x_B^j = j \cdot (W + V)$  is the position of the building. The summed error over all estimated buildings is given by

$$E(H_D) = \sum_{j=1}^M (\hat{z}_j - H_{Av}) \quad (15)$$

Note that buildings for which there is no tangent user cannot be directly estimated and are assigned the maximum height. Let us denote  $Q = \left\lfloor \frac{L}{W+V} \right\rfloor - M$  the number of such buildings. The total error over all buildings is now given by

$$\begin{aligned} E_T(H_D) &= Q \cdot (H_{Max} - H_{Av}) + \sum_{j=1}^M (\hat{z}_j - H_{Av}) \\ &= \left( \left\lfloor \frac{L}{W+V} \right\rfloor - M \right) \cdot (H_{Max} - H_{Av}) + \sum_{j=1}^M \frac{W \cdot (H_D - H_{Av})}{2j(W+V)} \end{aligned} \quad (16)$$

A suitable UAV altitude  $H_D$  is found via the following line search

$$\begin{aligned} \min_{H_D} E_T(H_D) \\ s. t. : Q \geq 0 \end{aligned} \quad (17)$$

## V. NUMERICAL RESULTS

We consider a dense urban Manhattan-like 1 km by 1 km area consisting of a regular street grid and buildings with

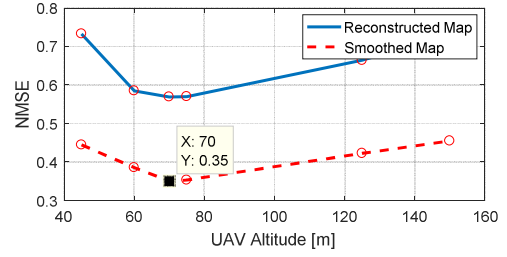


Fig. 6. Reconstruction NMSE for both smoothed and rough map versus different UAV elevations.

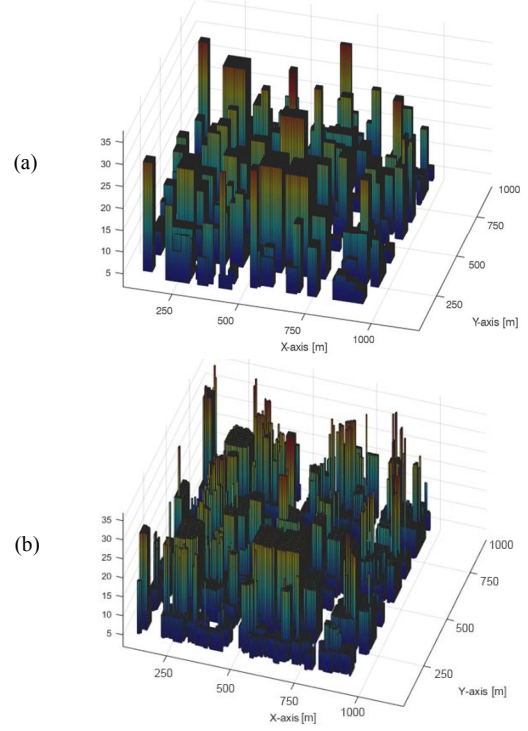


Fig. 7. (a) Side view of the 3D city map. The city map is discretized over small grid squares of length of 5 meters. (b) Reconstructed map after refinement and smoothing with NMSE equals to 0.35.

uniform random height in the range of  $H_{Min}=5$  to  $H_{Max} = 40$  meters. The width of each building is random uniform with average  $W = 80$  meters and the main street width is set to  $V = 60$  meters. The outdoor users are spread uniformly randomly as in Fig. 1. For reconstruction purposes, the map is discretized over a grid with 5 meters granularity. The UAV test trajectory is a square with length 800 meters, centered at the center of the map.  $K = 32$  set of measurements are reported (every 100 meters). Propagation parameters are chosen as  $\alpha_{LoS} = 2.27$ ,  $\beta_{LoS} = -40$ ,  $\alpha_{NLoS} = 3.64$ ,  $\beta_{NLoS} = -30$  generalized from typical fixed base station WINNER II [17]. Finally we select  $\sigma_{LoS}^2 = 2$ ,  $\sigma_{NLoS}^2 = 5$ .

To further improve reconstruction performance, a map smoothing procedure is used, whose goal is to filter out unrealistic height variations among closely located points on the grid. Due to lack of space, the details of the smoothing filter are explained in an upcoming companion paper.

We first test the target group selection optimization method of Section III. Results are shown in Fig. 4 which confirms the classification error to be minimized at the ring radius predicted by our algorithm.

In Fig. 5 the classification result using K-means for users in the target area is depicted. The users are almost fully distinguishable, note that the signals with higher RSSI are LoS users. Then using SVM classifier all users ( $N = 1584$ ) are classified with 99.9% precision which indicates a good performance of the classifier for our purpose.

Next, we are interested in optimal flying altitude and run the optimization in (17) to find a best altitude at 70 meters. The prediction is tested in Fig. 6 which shows the reconstruction error for a range of UAV altitudes, also predicting an optimum near 70 meters.

Fig. 7 shows an instance of reconstructed map after smoothing for the considered flight path with fixed altitude  $H_D = 70$  meters. Note that, for the regions where there is no user reportings, the building estimated heights are set to the average building height by default.

Finally, the impact of user density is tested in Fig. 8 showing the improvement trend as the number of users (hence RSSI reportings) increase.

## VI. CONCLUSIONS

This paper considers the problem of 3D city map reconstruction by exploitation of UAV-bound radio measurements. The proposed approach relies on the unique ability for a UAV-to-ground communication systems to detect and classify line-of-sight (LoS) vs. non line-of-sight (NLoS) channels towards ground users using machine learning tools. The optimal height for the UAV is found using an analytical model which shows excellent predictive behavior. The present algorithm assumes perfect LoS/NLoS classification. In the case classification error statistics are available, robust approaches based on Bayesian estimation can be developed which are reported in companion work.

## REFERENCES

- [1] Zhang, Zuxun, et al. "Multi-view 3D city model generation with image sequences." INTERNATIONAL ARCHIVES OF PHOTOGRAMMETRY REMOTE SENSING AND SPATIAL INFORMATION SCIENCES 34.5/W12 (2003): 351-356.
- [2] Zhou, Qian-Yi, and Ulrich Neumann. "Complete residential urban area reconstruction from dense aerial LiDAR point clouds." Graphical Models 75.3 (2013): 118-125.
- [3] Savarese, Silvio. "Shape reconstruction from shadows and reflections." PhD diss., California Institute of Technology, 2005.
- [4] Y. Zeng, R. Zhang, and T. J. Lim, "Wireless communications with unmanned aerial vehicles: opportunities and challenges," IEEE Commun. Mag., vol. 54, no. 5, pp. 36–42, 2016.
- [5] M. Mozaffari, W. Saad, M. Bennis, and M. Debbah, "Drone small cells in the clouds: Design, deployment and performance analysis," in Proc. IEEE Global Telecomm. Conf., 2015, pp. 1–6.

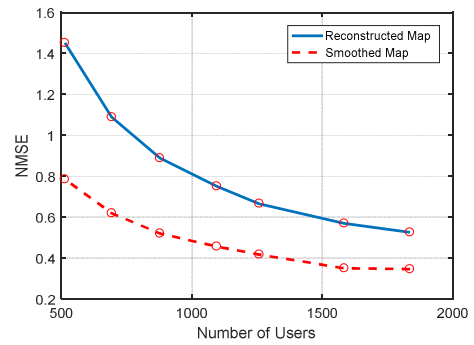


Fig. 8. Map reconstruction error versus increasing the number of users.

- [6] J. Chen, D. Gesbert, "Optimal Positioning of Flying Relays for Wireless Networks: A LOS Map Approach", in Proc. of the International Conference on Communications (ICC), Paris, May 2017.
- [7] Choi, Dae Hyung, Byoung Hoon Jung, and Dan Keun Sung. "Low-complexity maneuvering control of a UAV-based relay without location information of mobile ground nodes." Computers and Communication (ISCC), 2014 IEEE Symposium on. IEEE, 2014.
- [8] Z. Becvar, M. Vondra, P. Mach, J. Plachy, "Performance of Mobile Networks with UAVs: Can Flying Base Stations Substitute Ultra-Dense Small Cells?", in Proceedings of European Wireless, Dresden, 2017.
- [9] J.Chen, U. Yatmali, D. Gesbert, "Learning radio Maps for UAV-aided Wireless Networks: A Segmented regression Approach", in IEEE Int. Conf. Commun., 2017.
- [10] Romero, D., Kim, S.J., Giannakis, G.B. and Lopez-Valcarce, R., 2016. Learning Power Spectrum Maps from Quantized Power Measurements. arXiv preprint arXiv:1606.02679.
- [11] Al-Hourani, Akram, Sithamparamathan Kandeepan, and Abbas Jamalipour. "Modeling air-to-ground path loss for low altitude platforms in urban environments." Global Communications Conference (GLOBECOM), 2014 IEEE. IEEE, 2014.
- [12] Ostlin, Erik, Hans-Jürgen Zepernick, and Hajime Suzuki. "Macrocell path-loss prediction using artificial neural networks." IEEE Transactions on Vehicular Technology 59.6 (2010): 2735-2747.
- [13] MacQueen, James. "Some methods for classification and analysis of multivariate observations." Proceedings of the fifth Berkeley symposium on mathematical statistics and probability. Vol. 1. No. 14. 1967.
- [14] DeSarbo, Wayne S., and William L. Cron. "A maximum likelihood methodology for clusterwise linear regression." Journal of classification 5.2 (1988): 249-282.
- [15] Xiao, Zhuoling, et al. "Identification and mitigation of non-line-of-sight conditions using received signal strength." Wireless and Mobile Computing, Networking and Communications (WiMob), 2013 IEEE 9th International Conference on. IEEE, 2013.
- [16] Manning, Christopher D., Prabhakar Raghavan, and Hinrich Schütze. Introduction to information retrieval. Vol. 1. No. 1. Cambridge: Cambridge university press, 2008.
- [17] Winner II interim channel models,"Tech. Rep. IST-4-027756 WINNER II D1.1.2 v1.2, Sept. 2007.
- [18] J. Chen, O. Esrafilian, D. Gesbert, and U. Mitra. "Efficient Algorithm of Air-to-ground Channel Reconstruction for UAV-aided Communications." Globecom Workshop on Wireless Networking and Control for Unmanned Autonomous Vehicles, 2017 IEEE.
- [19] Irish, Andrew T., et al. "Probabilistic 3D mapping based on GNSS SNR measurements." Acoustics, Speech and Signal Processing (ICASSP), 2014 IEEE International Conference on. IEEE, 2014.
- [20] Karanam, Chitra R., and Yasamin Mostofi. "3D through-wall imaging with unmanned aerial vehicles using wifi." Proceedings of the 16th ACM/IEEE International Conference on Information Processing in Sensor Networks. ACM, 2017.